Desalination and Water Treatment
www.deswater.com

doi: 10.5004/dwt.2017.20393

63 (2017) 135–144
February

Development of new hybrid nanosorption/ceramic microfiltration for Cu(II) removal

Wanida Chooaksorn, Rachnarin Nitisoravut*

School of Bio-Chemical Engineering and Technology, Sirindhorn International Institute of Technology, Thammasat University, Pathum Thani 12121, Thailand, Tel. +66 (0) 2986 9009 Ext. 2304; Fax: +66 (0) 2986 9009 Ext. 2315; emails: snitisor@siit.tu.ac.th (R. Nitisoravut), chooaksorn@hotmail.com (W. Chooaksorn)

Received 1 April 2016; Accepted 25 August 2016

ABSTRACT

A new technique has been developed for Cu(II) removal using simultaneous filtration and adsorption by coating modified nanochitosan on a ceramic microfiltration membrane. It offers continuous operation and ease of chitosan nanoparticle usage without flow retardation. In this work, nanochitosan (CMCN), nanochitosan cross-linked with glutaraldehyde (CMCN-GLA), and polyethylene glycol (CMCN-PEG) were coated onto a microfiltration ceramic membrane, and then tested for Cu(II) removal performance. Among the three materials tested, CMCN-GLA provided the highest adsorption capacity of 240.3 mg/g at a flow rate of 2.5 mL/min. It is greater than a 30% improvement of adsorption capacity, as compared with native nanochitosan. This is about 2.4 times higher than a previous study on simultaneous adsorption-filtration. The experimental data was found to fit well with the Thomas model.

Keywords: Breakthrough curve; Ceramic membrane; Chitosan; Metal removal; Nano-adsorbent; Thomas model

1. Introduction

Heavy metals in the environment may be attributed to an improper discharge and inadequate treatments of wastewater from various industries such as metal finishing, battery manufacturing, electrical cables, and mining industries [1–3]. The heavy metals of concern include cadmium, chromium, mercury, copper, and lead [4]. Copper (Cu(II)) is an important trace element for the health of humans, plants, and animals. However, overexposure to Cu(II) leads to acute effects such as abdominal pain, headache, nausea, dizziness, vomiting, diarrhea, and cancer [5,6]. Many techniques have been developed for Cu(II) removal from wastewater [7–9]. Of these techniques, adsorption is the most prominent and effective method for Cu(II) separation from wastewater [10]. Nevertheless, the adsorption process regularly needs an additional step to separate an adsorbent from treated wastewater.

Chitosan is an outstanding adsorbent for Cu(II) adsorption, even at low concentrations [11]. It can be modified by many chemicals to improve its properties and extend its applications, such as cross-linking using epichlorohydrin, formaldehyde, or glutaraldehyde (GLA) and graft copolymerization with polyethylene glycol (PEG), vinyl acetate, acrylonitrile, or polystyrene [12–16]. Graft copolymerization is an effective method to enhance water solubility, chelating, adsorption capacity, selectivity, antibacterial, and antioxidant properties. There are two positions to graft onto chitosan, which are covalent binding with hydroxyl groups on acetylated or deacetylated chitosan, and free amine groups on deacetylated chitosan [17]. Moreover, there are three initiating methods, which are chemical initiation, radiation initiation, and enzyme initiation [13,18,19]. Several researchers reported that the solubility in water of chitosan-grafted copolymer with PEG depends on PEG molecular weight, weight ratio of PEG, degrees of N-substitution, and degree of deacetylation [20]. Kim et al. [21] studied the behavior of

* Corresponding author.

modified chitosan, poly N-isopropylacrylamide-grafted chitosan cross-linked with GLA, and reported that the modified chitosan can be thermo- and pH-sensitive, which may affect its applications. The possible use of chitosan has attracted much attention for the use of its nano-scale particles. Several studies have also used nanochitosan in the development of drug delivery.

However, there are limited numbers of studies that have reported on chitosan nanoparticles (CN) for wastewater treatment. This is because of their unique properties of nanometer sizes, high specific surface area, high surface functional groups, and high potential for metal binding. Moreover, CN are biocompatible, with no known toxicity to human and environment. These properties would benefit large-scale environmental applications, particularly heavy metal removal from wastewater treatment [22–24].

Membrane filtration is widely used for heavy metals removal, particularly ultrafiltration, nanofiltration, reverse osmosis, and electrodialysis [25]. Membranes have great ability for heavy metal removal, high permeate fluxes, convenient operation, and space savings [25,26]. Moreover, using membrane filtration allows continuous operation and can be simply integrated with other methods [3,26].

The combination of adsorption and membrane filtration is of interest. In this study, a ceramic microfiltration membrane was used as a filter and support material for nanochitosan. In order to shorten the treatment process and to enhance the Cu(II) removal, nanochitosan was coated on the surface of a membrane, resulting in simultaneous filtration and adsorption on the membrane surface [18]. Moreover, the ceramic membrane (CM) provides the support for CN and removes the difficulty associated with filtration of nanoparticles, as well as facilitates the reuse and regeneration of the nanochitosan [27]. Chelation was used to overcome the mass transfer limitations by coating biosorbents, nanochitosan, and modified chitosan GLA and PEG, on the surface of CMs. Their efficiencies for Cu(II) adsorption were explored. Continuous flow adsorption studies were conducted to obtain breakthrough curves and to evaluate the membrane adsorption performance by using a kinetic model.

2. Materials and methods

2.1. Chemicals and materials

Chitosan flakes with average molecular weight 50 kDa, size of 1–3 mm, and 85% deacetylation were obtained from Bio 21 Co. Ltd, Chonburi (Thailand). All the chemicals used were of analytical grade. Acetic acid, copper nitrate tetrahydrate ($Cu(NO_3)_2{\cdot}3H_2O$, 99.9%), sodium tripolyphosphate (TPP, 99.9%), GLA (25%), polyethelene glycol (PEG), sodium hydroxide (NaOH), sulfuric acid (H_2SO_4), and hydrochloric acid (HCl) were manufactured by Merck, Thailand. All glassware was washed with 1:1 nitric acid (HNO_3, 65%) from Carlo Erba, Thailand. The working standard solutions of 1,000 mg/L Cu(II) were prepared by dissolving $Cu(NO_3)_2{\cdot}3H_2O$ in deionized water (DI water). Standard solutions at other concentrations were prepared with dilutions from the prepared stock solution.

A cross-flow microfilter was obtained from Tami Industries (Germany). It was made of ZrO_2-TiO_2 composite, 250-mm length, 6-mm internal diameter, and 10-mm outer diameter. The membrane has a nominal pore diameter of 0.45 μm and an effective surface area of 0.0047 m^2.

2.2. Adsorbent preparation

2.2.1. Preparation of chitosan nanoparticles

CN were prepared according to the ionic gelation method with TPP as an ionic cross-linker [28]. A homogeneous solution of chitosan was prepared by dissolving 200 mg of chitosan flake in 200 mL of 1% acetic acid. This was stirred for 2 h. at room temperature until all flakes were dissolved. A TPP solution (1.0 mg/mL, 25 mL) was gradually added to the solution at a rate of 1.0 mL/min, at a mixing speed 1,200 rpm. The process is based on the interaction between the negatively charged phosphate groups of the TPP and the positively charged amino groups of chitosan. TPP, which has three phosphate groups, can interact with the amino groups on several locations of the chitosan chains, leading to the formation of the nanoparticle size colloids [29].

2.2.2. Preparation of cross-linked chitosan nanoparticles

To increase the stability and binding properties of these CN, they were further modified, using either GLA or PEG as follows:

(a) Chitosan nanoparticles-glutaraldehyde (CN-GLA): CN can be further cross-linked using GLA. The 0.5 mL of 25% GLA solution was added to the CN solution at an average mixing speed of 1,200 rpm for 2 h.
(b) Chitosan nanoparticles-polyethylene glycol (CN-PEG): PEG (200 mg) was added to 250 mL of CN solution and mixed thoroughly using a magnetic stirrer at a mixing speed of 1,200 rpm for 2 h.

2.3. Coating of nanochitosan onto ceramic membrane

Firstly, a CM was cleaned with DI water. Then it was burned in a hot-air furnace at 600°C in order to remove any organic residuals that remain. After cooling to room temperature, the membrane was then coated with the selected chitosan solutions (CN, CN-GLA, or CN-PEG) by immersing the membrane into the solution for 2 min, followed by drying at 60°C in an oven for 15 min. The 2-min coating was selected from the preliminary tests (not shown). A coating time beyond 2 min did not result in much increase in the amount of CN coated onto the membrane. This step was repeated ten times in order to coat a sufficient amount of chitosan onto the CM. Finally, the coated membrane was dried at 60°C for 1 h. and stored in a desiccator prior to use.

The thickness of membrane-coated layer (CMCN, CMCN-GLA, and CMCN-PEG) was evaluated based on Eq. (1) [30,31]. Weights of the membrane before and after depositions were determined:

$$L = \frac{m_2 - m_1}{Ap(1-\varepsilon)} \quad (1)$$

where L is the membrane thickness; m_1 is the mass of membrane support ZrO_2-TiO_2; m_2 is the total mass of the support and the coated CN; A is the membrane area (0.0047 m^2);

p is the theoretical density of ZrO_2-TiO_2 (5.68 g/cm^3); and ε the assumed porosity of the membrane (25%).

2.4. Characterization methods

The CN were characterized for their morphologies and sizes using an atomic force microscope (AFM) (Seiko Instrument Model SPI 4000). Morphology of the CM, coated with various adsorbents, was characterized by a scanning electron microscope (SEM; Hitachi Model S-3400N) and field emission scanning electron microscope (FE-SEM) (JEOL Model JSM-7800F). Elemental and chemical analyses were examined by an Oxford energy dispersive spectrometer (EDS/EDX; LINK ISIS200). The equilibrium concentration of Cu(II) was determined by using an atomic absorption spectrophotometer (AAS; Perkin Elmer Analyst 200). A pH meter (Mettler Toledo Model SG2-SevenGo™) was used to measure pH.

2.5. Experimental setup and procedure

The pilot unit used for adsorption-microfiltration experiments is illustrated in Fig. 1. The unit was designed as a single-channel tubular membrane. It was equipped with a feed tank, rotameters, control and drain valves, pressure gauges, and a feed pump. The feed tank was filled with Cu(II) solution. Permeation and adsorption tests were performed at a gauge pressure of 1 psi.

The adsorption-microfiltration performance was studied with a control experiment without adsorbents. Samples of feed, retentate, and permeate were collected at various time intervals. The Cu(II) adsorption and water permeation through the adsorbent-coated CM were measured.

The permeate flux (L/m^2·h) was calculated using Eq. (2) [32]:

$$J = \frac{Vp}{A\Delta t} \tag{2}$$

where J is permeate flux (L/m^2·h); Vp is volume of permeate (L); A is active surface area of membrane (m^2); and Δt is time collecting the permeate (h).

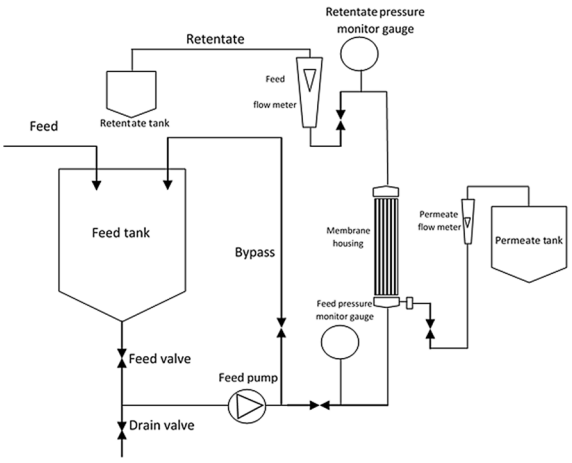

Fig. 1. Experimental setup used for adsorption-microfiltration experiment.

The amount of Cu(II) bound to the adsorbent, or uptake capacity (q_e, mg/g), can be calculated by using Eqs. (3) and (4) [33,34]:

$$q_{\text{total}} = \frac{Q}{1000}\int_{t=0}^{t=t_{\text{total}}} (C_0 - C_t)dt \tag{3}$$

$$q_{e,\max} = \frac{q_{\text{total}}}{m} \tag{4}$$

where q_{total} is equal to the area under the plot of the adsorbed heavy metal concentration vs. time (mg); $q_{e,\max}$ is the maximum adsorption capacity (mg/g); Q is the flow rate (mL/min); C_0 and C_t are concentrations (mg/L) at initial and at set times, respectively; and m is the mass of the adsorbent (mg).

Cumulative mass of Cu(II) adsorbed (mg/g) is the total amount of Cu(II) adsorbed onto the chitosan calculated from the decrease in the Cu(II) concentration in the solution multiplied with the volume of the permeate collected up to that run.

The breakthrough curves and the adsorption kinetics of the membrane performance were analyzed using the Thomas model. The Thomas model is based on a single resistance mass transfer and is frequently employed to describe fixed-bed adsorption where the external mass transfer is the rate-limiting step [35]. The linear equation of the Thomas model is given as follows [36–38]:

$$\ln\left(\frac{C_0}{C_t} - 1\right) = \frac{k_{Th} q_0 M}{Q} - k_{Th} C_0 t \tag{5}$$

where k_{Th} is the adsorption rate constant (mL/mg·min); q_0 is the adsorption capacity (mg/g); M is the mass of adsorbent (mg); Q is the feed flow rate (mL/min); C_0 and C_t are the initial and effluent concentrations (mg/L), respectively; and t is the total flow time (min). A linear plot of $\ln(C_0/C_t - 1)$ vs. t can be used to obtain the adsorption rate constant (k_{Th}) and the adsorption capacity of the sorbent (q_0).

2.6. Membrane desorption

After the membrane was saturated, which is defined as when there was no further change in Cu(II) concentration flowing through the system, the adsorbed Cu(II) was then desorbed with 0.1 M H_2SO_4 solution at a flow rate of 10 mL/min. After desorption, the adsorption was repeated. The adsorption-desorption of Cu(II) was repeated for three consecutive cycles.

The percentage desorption is expressed in Eq. (6):

$$\%\ \text{Desorption} = \frac{\text{Cu}_{\text{ads}} - \text{Cu}_{\text{des}}}{\text{Cu}_{\text{ads}}} \times 100 \tag{6}$$

where Cu_{ads} is the amount of Cu(II) adsorbed (mg), calculated using Eq. (3), but without division by the sorbent mass, and Cu_{des} is the amount of Cu(II) desorbed (mg), calculated from the concentration of Cu(II) in the desorbed solution.

3. Results and discussion

3.1. Characterizations of ceramic membrane surface

The size ranges of CN were estimated to be about 25–80 nm, which were measured by an AFM (Fig. 2(a)). The figure indicates the spherical shape of CN on the surface of the CM. Also, the FE-SEM image of the CN (Figs. 2(b) and (c)) supports the AFM results. The adsorbents (CN, CN-GLA, and CN-PEG) were deposited onto the surface of the CM. This was to a thin layer of chitosan on the ceramic surface to functionalize the membrane, thereby preparing the surface for chemical modification [39]. Fig. 3 shows the morphology of the CM surface with the three adsorbents, characterized by SEM. Fig. 3(a) depicts the clear and coarse surface of the bare CM. The surface, when covered with CN, became thicker and smoother (Fig. 3(b)). Figs. 3(c) and (d) indicate the coatings of the CM with CMCN-GLA and CMCN-PEG, resulting in significant changes in the surface morphology, from a coarse to smooth film-like morphology.

The difference of dried mass of the CM before and after adsorbent depositions on the surface was used to calculate the amount of adsorbent coated on the membrane. Fig. 4 shows the thickness of CMCN, CMCN-GLA, and CMCN-PEG, coated on the membrane, calculated according to Eq. (2), which was 0.572, 0.669, and 0.692 μm, respectively. The thickness of CMCN-PEG on the ceramic surface was the highest, probably due to the binding properties of PEG 1000. However, increasing the PEG amount may not always lead to thicker coating. Bhattarai et al. [40] and Hou et al. [41] investigated the grafting of PEG onto chitosan and observed that due to the hydrophilic nature of PEG, the resulting polymer may be able to dissolve in water better than the parent chitosan. Increasing the amount of PEG in the coating may therefore lead to the dissolution of the coating, which may not be a desirable property here. Based on the previous study on modified chitosan, GLA-cross-linked chitosan is more hydrophobic than native chitosan [42].

The chemical composition of the CM with various adsorbents, as determined by EDS, is presented in Fig. 5. Fig. 5(a) shows that the peaks assigned to Ti and O were dominant (more than 90% of the total composition) for the CM. The EDS composition after Cu(II) adsorption provides the

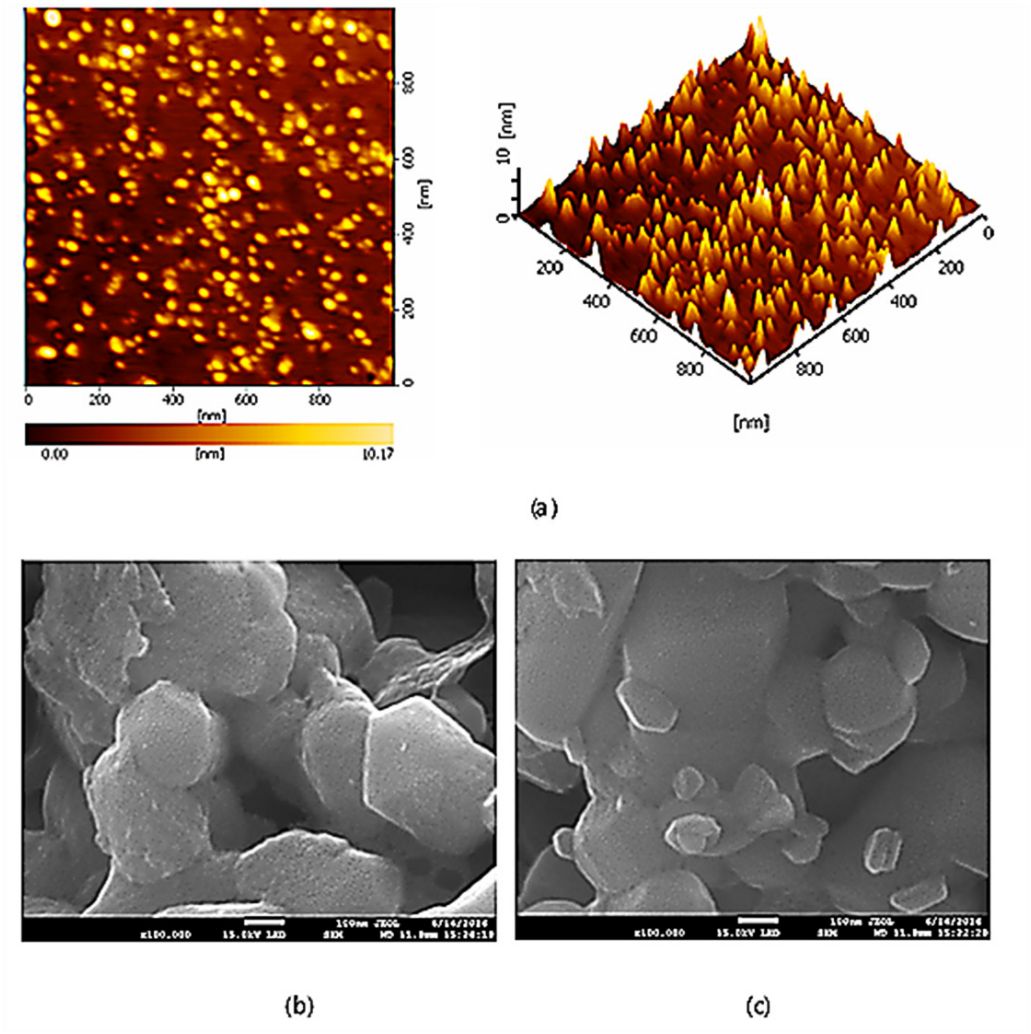

Fig. 2. (a) AFM images show the topographic and three-dimensional image of CN; (b) FE-SEM surface image of CM; and (c) FE-SEM image of CN coated on the surface of CM.

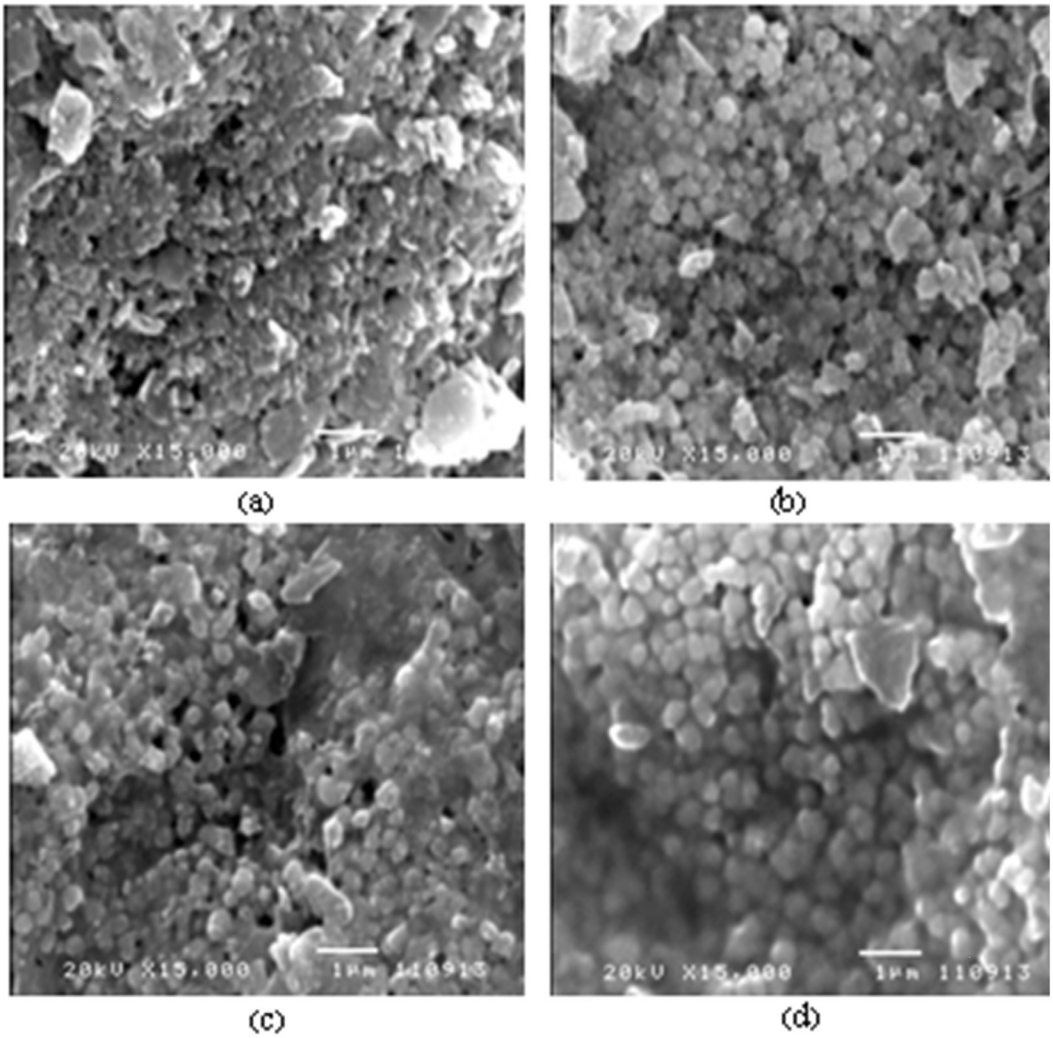

Fig. 3. SEM images: (a) CM; (b) CMCN; (c) CMCN-GLA; and (d) CMCN-PEG.

composition of Ti, C, and O, which were major constituents of chitosan and the CM. Figs. 5(b)–(d) show direct evidence for Cu(II) uptake by various adsorbents after adsorption (0.32%, 0.85%, and 0.16% by weight with CMCN, CMCN-GLA, and CMCN-PEG, respectively).

3.2. Cu(II) removal

The achievements of simultaneous removal of Cu(II) by filtration and adsorption are illustrated in Fig. 6. Cu(II) was unable to be removed by the bare CM, but can be adsorbed by the interaction with nanochitosan and modified nanochitosan. Cu(II) removal, up to 89.38%, was accomplished by CMCN-GLA, at a flow rate 2.5 mL/min (Fig. 6(a)). The specific adsorption capacity (mg Cu/g chitosan) was 240.3 mg/g, which is 2.4 times higher when compared with the simultaneous adsorption-filtration study using native chitosan by Steenkamp et al. [43]. When the flow rate was doubled to 5.0 mL/min, the specific adsorption capacity decreased to 222.1 mg/g chitosan. At a higher flow rate, a greater amount of Cu(II) passed by the adsorbent, resulting in increased Cu(II)

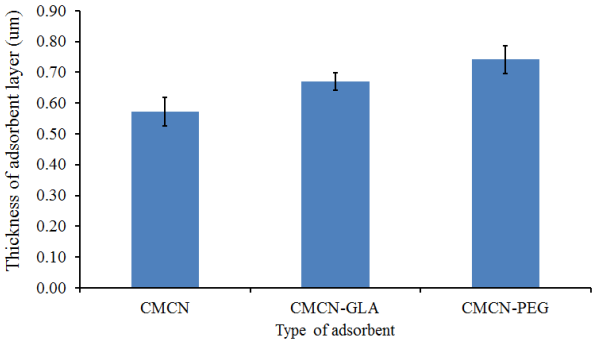

Fig. 4. Thickness of adsorbent on ceramic membrane.

on the sorbent. For CMCN and CMCN-PEG, at a flow rate of 2.5 mL/min, the removal was achieved with specific adsorption capacity of 182.0 and 100.7 mg/g of chitosan, respectively. The adsorption capacity decreased to 159.2 and 84.0 mg/g, respectively, at a flow rate of 5.0 mL/min for CMCN

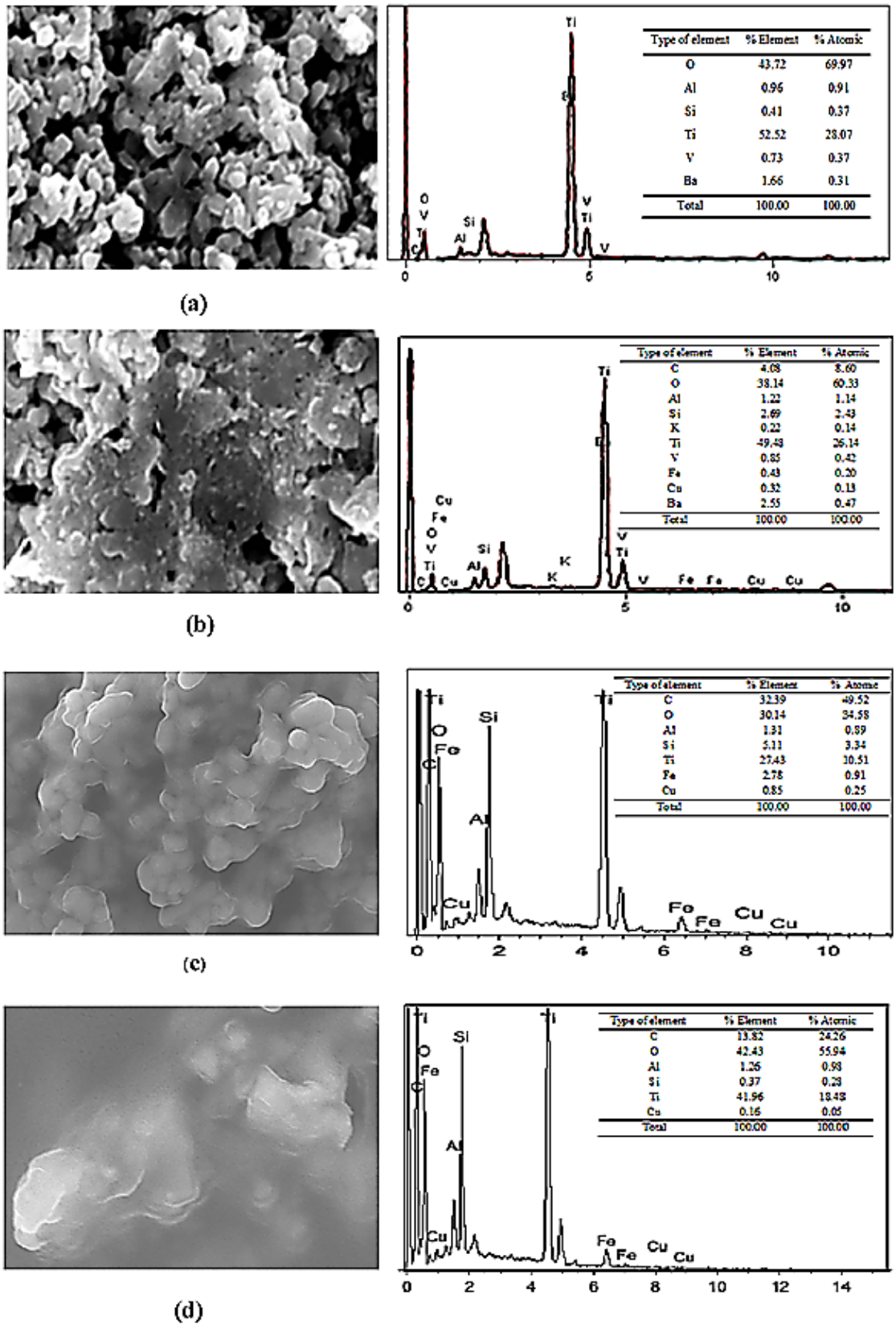

Fig. 5. SEM images of ceramic membrane surface coated with different adsorbents after Cu(II) adsorption at 15,000X, and EDS analysis: (a) CM; (b) CMCN; (c) CMCN-GLA; and (d) CMCN-PEG.

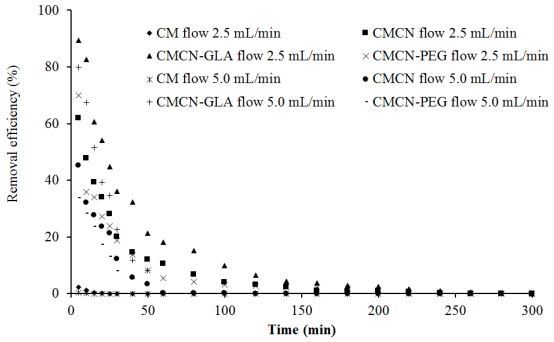

(a)

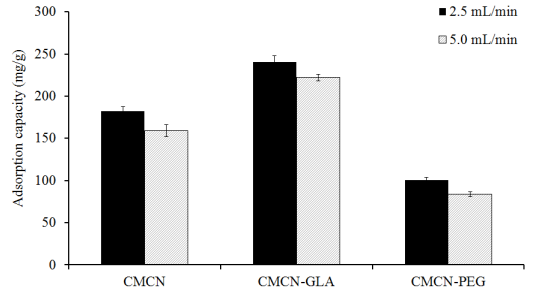

(b)

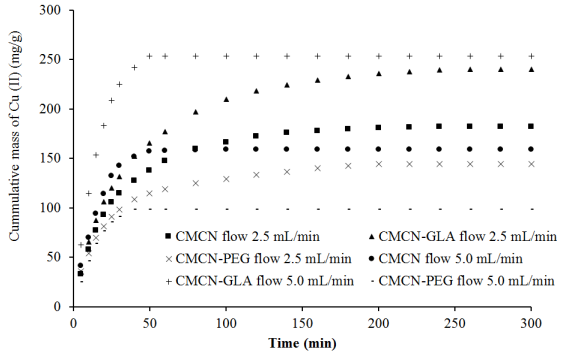

(c)

Fig. 6. Adsorption of Cu(II) by various adsorbents, coated on the ceramic membrane for different flow rates: (a) time course of Cu(II) removal efficiency; (b) adsorption capacity of Cu(II); and (c) cumulative Cu(II) mass with time.

and CMCN-PEG (Fig. 6(b)). When the surface of the membrane changes from a particle-like morphology to a film-like morphology, the adsorption rate decreased as the surface area also decreased. The decreased percentage and adsorption capacity can be attributed to the insufficient time for Cu(II) diffusion into the inner pores of the adsorbent [7,44].

Moreover, nanochitosan is more hydrophobic and can also play an active role in Cu(II) sorption via free aldehyde groups. This is because the chemical modification with GLA [42] results in negative species to bind with Cu(II) [37,45]. Although a chitosan-grafted copolymer with PEG can be used to recover cations from solution [46], this results in greater water solubility, and therefore, there could be swelling [47,48]. However, note that the cumulative amount of Cu(II) adsorbed increased with an increase in flow rate, while the adsorption capacity (amount of Cu(II)/adsorbent loading) decreased. This result indicates that the sorption of Cu(II) took place primarily on the adsorbent surface. The Cu(II) adsorption started to level off after 60 min of operation, and then approached steady state conditions, after nearly 300 min of operation (Fig. 6(c)). It appears that rapid uptake of Cu(II) occurred at the beginning of operation, and the rate decreased thereafter and finally reached saturation.

A membrane study for three consecutive adsorption-desorption cycles shows the stability of coated adsorbents on the membrane surface and the ease of desorption. Desorption of adsorbents can be successfully accomplished for three consecutive cycles using 0.1 M H_2SO_4 solution. The mechanism of desorption involves H^+ from H_2SO_4. The bound Cu(II) undergoes both electrostatic and complexation reactions, affected by the ionic strength of solutions [45,49]. Thus, the electrostatic interaction between chitosan and Cu(II) becomes weaker, causing the release of adsorbed Cu(II) and the adsorption sites to be evacuated. Similar desorption data were also reported by Wambu et al. [50].

In addition, the membrane coating stability was evaluated based on the difference of the dry weight before and after use of the coated membrane. Assuming that the detachment during operation was the prime mechanism for weight loss, it was found that the coating adhered to the membrane surface quite well with most of the weight losses occurred during the initial flow. At the flow rate of 2.5 mL/min, the weight loss after 180 min of operation was about 15%. Additional loss of 3% occurred toward 300 min of run time. The loss of weight during initial flow was suspected to associate with the loose particles on the membrane surface. At higher flow rate of 5.0 mL/min, the weight loss was slightly larger of about 18% during the first 180 min. Increasing run time to 300 min caused only 2% further loss of weight.

3.3. Permeate flux

Fig. 7 shows the permeate flux evolution for various adsorbents coated on a CM. As indicated, the flux is inversely proportional to the thickness of adsorbent in the order of CM > CMCN > CMCN-GLA > CMCN-PEG. A rapid decline of flux occurred during the first 60 min and slowly decreased thereafter until 100 min, then relatively stabilized toward the end of the experiment at 300 min. This initial decrease in flux may be due to the swelling of chitosan, resulting in a reduced pore size and decreased flux from the initial values. After 100 min, a slight decrease in flux may be caused by membrane fouling and compaction. CMCN-PEG has the lowest permeate flux, which may be associated with a film-like morphology on the surface and the hydrophilicity of the PEG, causing large film swelling and reduced pore size [51]. The use of the hydrophilic polymer PEG may, therefore, offer good filtration, but with more resistance to flow. As reported by Jana et al. [52], a slow decrease of flux may be due to a thicker chitosan layer on the membrane surface, concentration polarization, and membrane fouling.

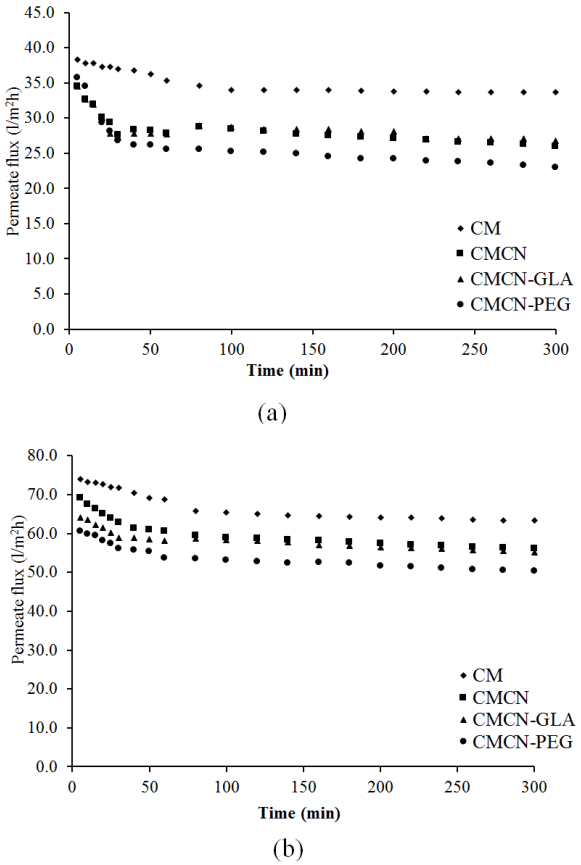

Fig. 7. Permeate flux of various adsorbents at: (a) 2.5 mL/min and (b) 5.0 mL/min.

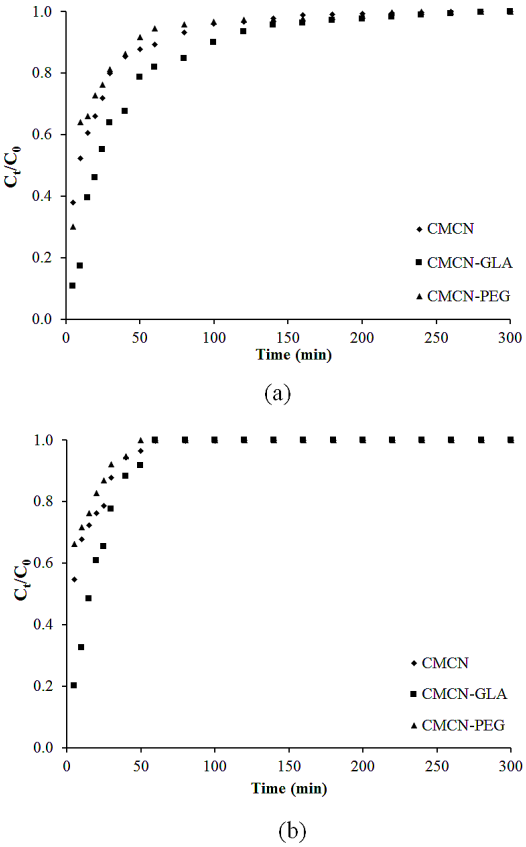

Fig. 8. Breakthrough curves for various adsorbents at: (a) 2.5 mL/min and (b) 5.0 mL/min.

3.4. Breakthrough curves

The profile and slope of the breakthrough curves, as indicated in Fig. 8, shows slight differences for the adsorbents. The CMCN-PEG saturated earlier than other adsorbents. The breakthrough times of all adsorbents decreased with an increase in flow rate. At a high flow rate, Cu(II) solution leaves the membrane before equilibrium occurs. There is insufficient contact time for Cu(II) adsorption, leading to a low removal efficiency and uptake capacity. [7,53,54]. This mechanism can be attributed to the fact that earlier saturation leads to a shorter breakthrough time [55]. The results indicate that there was an overflow of the adsorbate in the membrane at a flow rate exceeding 5.0 mL/min. The CMCN-GLA took a longer time to approach saturation. This result indicates that the sorption occurred mainly on the adsorbent surface.

3.5. Kinetic models

The kinetics study shows the adsorption capacity of Cu(II) onto several adsorbent-coated CMs, which is described by the Thomas model. The R^2 values are in a range of 0.920–0.990 and 0.880–0.972, at flow rates of 2.5 and 5.0 mL/min, respectively. The coefficient of determination and model parameters are presented in Table 1 with variation of adsorbents and flow rates. Noticeably, an increase of flow rate from 2.5 to 5.0 mL/min led to a reduction of adsorption capacity for all adsorbents. Although the Thomas model fits well all experimental types and flow rates, good prediction of adsorption capacity occurred only for CMCN and CMCN-GLA, at a low flow rate of 2.5 mL/min. The great discrepancy between the predicted and actual adsorption capacity for other absorbents was probably due to a high superficial velocity. For the CMCN-PEG, a poor prediction may be associated with its solubility, which results in detachment of adsorbent from the supported membrane.

The earlier saturation occurred at higher flow due to an increase of Cu(II) mass transfer from the liquid film to the adsorbent surface [7]. As the flow rate increased, the value of q_0 decreased while k_{Th} increased, which indicates that the mass transport resistance decreases as a result of different driving forces for adsorption between the adsorbent and Cu(II) [7,56]. This indicates that external or internal diffusion is not the limiting step of mass transfer. On the contrary, the mass transfer limiting step occurs in the first adsorption stage due to surface reactions [57].

Table 1
Characteristic parameters of the Thomas model for the adsorption of Cu(II) onto several adsorbents

Adsorbent	Flow rate (mL/min)	q_e (mg/g)	k_{Th} (mL/mg·min)	$q_{0,Th}$ (mg/g)	R^2
CMCN	2.5	182.0	0.00054	184.7	0.972
CMCN-GLA		240.3	0.00053	265.0	0.923
CMCN-PEG		100.7	0.00048	179.9	0.880
CMCN	5.0	159.2	0.00220	93.6	0.920
CMCN-GLA		222.1	0.00190	183.6	0.990
CMCN-PEG		84.0	0.00170	45.9	0.986

4. Conclusions

A new hybrid nanosorption/ceramic microfiltration membrane offers an alternative and efficient means for Cu(II) removal. The CM-coated CN, cross-linked with GLA, shows the highest adsorption capacity of 240.3 mg/g, for a flow rate 2.5 mL/min. The breakthrough curves were dependent on flow rate and illustrated good performance for CMCN-GLA. The experimental data correlated well with the Thomas model. The membrane parameters can be used for the design of treatment systems to remove Cu(II) from wastewater. Desorption studies show the three cycles of adsorption-desorption for CMCN, CMCN-GLA, and CMCN-PEG.

Acknowledgments

This work was supported by the Higher Education Research Promotion and National Research University Project of Thailand, Office of the Higher Education Commission and Sirindhorn International Institute of Technology graduate scholarship program, Thammasat University.

Abbreviations

CN — Chitosan nanoparticles
CMCN — Chitosan nanoparticles coated on ceramic membrane
CM — Ceramic membrane
CN-GLA — Chitosan nanoparticles-glutaraldehyde
CN-PEG — Chitosan nanoparticles-polyethylene glycol
CMCN-GLA — Chitosan nanoparticles-glutaraldehyde coated on ceramic membrane
CMCN-PEG — Chitosan nanoparticles-polyethylene glycol coated on ceramic membrane
TPP — Sodium tripolyphosphate

References

[1] M. Owlad, M.K. Aroua, W.A.W. Daud, S. Baroutian, Removal of hexavalent chromium-contaminated water and wastewater: a review, Water Air Soil Pollut., 200 (2009) 59–77.
[2] T. Panayotova, M. Dimova-Todorova, I. Dobrevsky, Purification and reuse of heavy metals containing wastewaters from electroplating plants, Desalination, 206 (2007) 135–140.
[3] Z. Wang, G. Liu, Z. Fan, X. Yang, J. Wang, S. Wang, Experimental study on treatment of electroplating wastewater by nanofiltration, J. Membr. Sci., 305 (2007) 185–195.
[4] W.S. Wan Ngah, L.C. Teong, M.A.K.M. Hanafiah, Adsorption of dyes and heavy metal ions by chitosan composites: a review, Carbohydr. Polym., 83 (2011) 1446–1456.
[5] R. Schmuhl, H.M. Krieg, K. Keizer, Adsorption of Cu(II) and Cr(VI) ions by chitosan: kinetics and equilibrium studies, Water SA, 27 (2001) 1–8.
[6] W.S. Wan Ngah, S. Fatinathan, Adsorption of Cu(II) ions in aqueous solution using chitosan beads, chitosan-GLA beads and chitosan-alginate beads, Chem. Eng. J., 143 (2008) 62–72.
[7] C.M. Futalan, C.-C. Kan, M.L. Dalida, C. Pascua, M.-W. Wan, Fixed-bed column studies on the removal of copper using chitosan immobilized on bentonite, Carbohydr. Polym., 83 (2011) 697–704.
[8] N. Sankararamakrishnan, P. Kumar, V. Singh Chauhan, Modeling fixed bed column for cadmium removal from electroplating wastewater, Sep. Purif. Technol., 63 (2008) 213–219.
[9] G.P. Kumar, P.A. Kumar, S. Chakraborty, M. Ray, Uptake and desorption of copper ion using functionalized polymer coated silica gel in aqueous environment, Sep. Purif. Technol., 57 (2007) 47–56.
[10] Y.-T. Zhou, H.-L. Nie, C. Branford-White, Z.-Y. He, L.-M. Zhu, Removal of Cu^{2+} from aqueous solution by chitosan-coated magnetic nanoparticles modified with α-ketoglutaric acid, J. Colloid Interface Sci., 330 (2009) 29–37.
[11] G. Crini, Non-conventional low-cost adsorbents for dye removal: a review, Bioresour. Technol., 97 (2006) 1061–1085.
[12] K.V. Harish Prashanth, R.N. Tharanathan, Chitin/chitosan: modifications and their unlimited application potential-an overview, Trends Food Sci. Technol., 18 (2007) 117–131.
[13] N.M. Alves, J.F. Mano, Chitosan derivatives obtained by chemical modifications for biomedical and environmental applications, Int. J. Biol. Macromol., 43 (2008) 401–414.
[14] M. Kong, X.G. Chen, K. Xing, H.J. Park, Antimicrobial properties of chitosan and mode of action: a state of the art review, Int. J. Food Microbiol., 144 (2010) 51–63.
[15] G. Crini, P.-M. Badot, Application of chitosan, a natural aminopoly saccharide, for dye removal from aqueous solution by adsorption process using batch studies: a review of recent literature, Prog. Polym. Sci., 33 (2008) 399–447.
[16] C. Li, J. Cui, F. Wang, W. Peng, Y. He, Adsorption removal of Congo red by epichlorohydrin-modified cross-linked chitosan adsorbent, Desal. Wat. Treat., 57 (2016) 14060–14066.
[17] N. Subhapradha, P. Ramasamy, A. Srinivasan, P. Madeswaran, V. Shanmugam, A. Shanmugam, Sulfation of β-chitosan and evaluation of biological activity from gladius of *Sepioteuthis lessoniana*, Int. J. Biol. Macromol., 62 (2013) 336–340.
[18] E. Guibal, Interactions of metal ions with chitosan-based sorbents: a review, Sep. Purif. Technol., 38 (2004) 43–74.
[19] R. Ramya, P. Sankar, S. Anbalagan, P.N. Sudha, Adsorption of Cu(II) and Ni(II) ions from metal solution using crosslinked chitosan-g-acrylonitrile copolymer, Int. J. Environ. Sci., 1 (2011) 1323–1338.
[20] M. Rinaudo, Chitin and chitosan: properties and applications, Prog. Polym. Sci., 31 (2006) 603–632.
[21] S.Y. Kim, S.M. Cho, Y.M. Lee, S.J. Kim, Thermo- and pH-responsive behaviors of graft copolymer and blend based on chitosan and N-isopropylacrylamide, J. Appl. Polym. Sci., 78 (2000) 1381–1391.

[22] M. Hua, S. Zhang, B. Pan, W. Zhang, L. Lv, Q. Zhang, Heavy metal removal from water/wastewater by nanosized metal oxides: a review, J. Hazard. Mater., 211–212 (2012) 317–331.
[23] X. Qu, P.J.J. Alvarez, Q. Li, Applications of nanotechnology in water and wastewater treatment, Water Res., 47 (2013) 3931–3946.
[24] X. Liu, Q. Hu, Z. Fang, X. Zhang, B. Zhang, Magnetic chitosan nanocomposites: a useful recyclable tool for heavy metal ion removal, Langmuir, 25 (2009) 3–8.
[25] F. Fu, Q. Wang, Removal of heavy metal ions from wastewaters: a review, J. Environ. Manage., 92 (2011) 407–418.
[26] E. Pongrácz, J. Landaburu-Aguirre, R. Keiski, V. García, Applicability of membrane technologies for the removal of heavy metals, Desalination, 200 (2006) 272–273.
[27] Z. Zhao, J. Zheng, M. Wang, H. Zhang, C.C. Han, High performance ultrafiltration membrane based on modified chitosan coating and electrospun nanofibrous PVDF scaffolds, J. Membr. Sci., 394–395 (2012) 209–217.
[28] M.S. Sivakami, T. Gomathi, J. Venkatesan, H.S. Jeong, S.K. Kim, P.N. Sudha, Preparation and characterization of nano chitosan for treatment wastewaters, Int. J. Biol. Macromol., 57 (2013) 204–212.
[29] L.-M. Zhao, L.-E. Shi, Z.-L. Zhang, J.-M. Chen, D.-D. Shi, J. Yang, Z.-X. Tang, Preparation and application of chitosan nanoparticles and nanofibers, Braz. J. Chem. Eng., 28 (2011) 353–362.
[30] X. Ding, Y. Fan, N. Xu, A new route for the fabrication of TiO_2 ultrafiltration membranes with suspension derived from a wet chemical synthesis, J. Membr. Sci., 270 (2006) 179–186.
[31] A.A. Babaluo, M. Kokabi, M. Manteghian, R. Sarraf-Mamoory, A modified model for alumina membranes formed by gel-casting followed by dip-coating, J. Eur. Ceram. Soc., 24 (2004) 3779–3787.
[32] Y. Zhu, S. Xia, G. Liu, W. Jin, Preparation of ceramic-supported poly(vinyl alcohol)–chitosan composite membranes and their applications in pervaporation dehydration of organic/water mixtures, J. Membr. Sci., 349 (2010) 341–348.
[33] E.I. Unuabonah, M.I. El-Khaiary, B.I. Olu-Owolabi, K.O. Adebowale, Predicting the dynamics and performance of a polymer–clay based composite in a fixed bed system for the removal of lead (II) ion, Chem. Eng. Res. Des., 90 (2012) 1105–1115.
[34] A. Tor, N. Danaoglu, G. Arslan, Y. Cengeloglu, Removal of fluoride from water by using granular red mud: batch and column studies, J. Hazard. Mater., 164 (2009) 271–278.
[35] Z. Yaneva, B. Koumanova, V. Meshko, Dynamic studies of nitrophenols adsorption on perfil in a fixed-bed column: application of single and two resistance model, Water Sci. Technol., 62 (2010) 883–891.
[36] P. Suksabye, P. Thiravetyan, W. Nakbanpote, Column study of chromium(VI) adsorption from electroplating industry by coconut coir pith, J. Hazard. Mater., 160 (2008) 56–62.
[37] J.T. Nwabanne, P.K. Igbokwe, Kinetic modeling of heavy metals adsorption on fixed bed column, Int. J. Environ. Res., 6 (2012) 945–952.
[38] P. Sivakumar, P.N. Palanisamy, Packed bed column studies for the removal of Acid Blue 92 and Basic Red 29 using non-conventional adsorbent, Indian J. Chem. Technol., 16 (2009) 301–307.
[39] C.J.M. Nova, D. Paolucci-Jeanjean, M.-P. Belleville, M. Barboiu, M. Rivallin, G. Rios, Elaboration, characterization and study of a new hybrid chitosan/ceramic membrane for affinity membrane chromatography, J. Membr. Sci., 321 (2008) 81–89.
[40] N. Bhattarai, H.R. Ramay, J. Gunn, F.A. Matsen, M. Zhang, PEG-grafted chitosan as an injectable thermosensitive hydrogel for sustained protein release, J. Controlled Release, 103 (2005) 609–624.
[41] S. Hou, L.K. McCauley, P.X. Ma, Synthesis and erosion properties of PEG-containing polyanhydrides, Macromol. Biosci., 7 (2007) 620–628.
[42] M.M. Beppu, R.S. Vieira, C.G. Aimoli, C.C. Santana, Crosslinking of chitosan membranes using glutaraldehyde: effect on ion permeability and water absorption, J. Membr. Sci., 301 (2007) 126–130.
[43] G.C. Steenkamp, H.W.J.P. Neomagus, H.M. Krieg, K. Keizer, Centrifugal casting of ceramic membrane tubes and the coating with chitosan, Sep. Purif. Technol., 25 (2001) 407–413.
[44] M.M. Sekhula, J.O. Okonkwo, C.M. Zvinowanda, N.N. Agyei, A.J. Chaudhary, Fixed bed column adsorption of Cu (II) onto maize tassel-PVA beads, J. Chem. Eng. Process Technol., 3 (2012) 1–5.
[45] R.S. Vieira, M.M. Beppu, Mercury ion recovery using natural and crosslinked chitosan membranes, Adsorption, 11 (2005) 731–736.
[46] N.S. Behbahani, K. Rostamizadeh, M.R. Yaftian, A. Zamani, H. Ahmadi, Covalently modified magnetite nanoparticles with PEG: preparation and characterization as nano-adsorbent for removal of lead from wastewater, J. Environ. Health Sci. Eng., 12 (2014) 1–11.
[47] M.J. Zohuriaan-Mehr, Advances in chitin and chitosan modification through graft copolymerization: a comprehensive review, Iran. Polym. J., 14 (2005) 235–265.
[48] H. Tanuma, T. Saito, K. Nishikawa, T. Dong, K. Yazawa, Y. Inoue, Preparation and characterization of PEG-cross-linked chitosan hydrogel films with controllable swelling and enzymatic degradation behavior, Carbohydr. Polym., 80 (2010) 260–265.
[49] N. Sankararamakrishnan, A. Dixit, L. Iyengar, R. Sanghi, Removal of hexavalent chromium using a novel cross linked xanthated chitosan, Bioresour. Technol., 97 (2006) 2377–2382.
[50] E.W. Wambu, G.K. Muthakia, P.M. Shiundu, K.J.W. Thiongo, Kinetics of copper desorption from regenerated spent bleaching earth, Am-Euras. J. Sci. Res., 4 (2009) 317–323.
[51] B.K. Nandi, R. Uppaluri, M.K. Purkait, Effects of dip coating parameters on the morphology and transport properties of cellulose acetate–ceramic composite membranes, J. Membr. Sci., 330 (2009) 246–258.
[52] S. Jana, A. Saikia, M.K. Purkait, K. Mohanty, Chitosan based ceramic ultrafiltration membrane: preparation, characterization and application to remove Hg(II) and As(III) using polymer enhanced ultrafiltration, Chem. Eng. J., 170 (2011) 209–219.
[53] R. Han, L. Zou, X. Zhao, Y. Xu, F. Xu, Y. Li, Y. Wang, Characterization and properties of iron oxide-coated zeolite as adsorbent for removal of copper(II) from solution in fixed bed column, Chem. Eng. J., 149 (2009) 123–131.
[54] K. Vijayaraghavan, J. Jegan, K. Palanivelu, M. Velan, Removal of nickel(II) ions from aqueous solution using crab shell particles in a packed bed up-flow column, J. Hazard. Mater., 113 (2004) 223–230.
[55] S. Chen, Q. Yue, B. Gao, Q. Li, X. Xu, K. Fu, Adsorption of hexavalent chromium from aqueous solution by modified corn stalk: a fixed-bed column study, Bioresour. Technol., 113 (2012) 114–120.
[56] N. Chen, Z. Zhang, C. Feng, M. Li, R. Chen, N. Sugiura, Investigations on the batch and fixed-bed column performance of fluoride adsorption by Kanuma mud, Desalination, 268 (2011) 76–82.
[57] Z. Aksu, F. Gönen, Biosorption of phenol by immobilized activated sludge in a continuous packed bed: prediction of breakthrough curves, Process Biochem., 39 (2004) 599–613.